Flow Development Through Interturbine Diffusers

R. G. Dominy

D. A. Kirkham

University of Durham,
School of Engineering,
Durham, United Kingdom

A. D. Smith
Rolls-Royce plc
Derby, United Kingdom

Interturbine diffusers offer the potential advantage of reducing the flow coefficient in the following stages, leading to increased efficiency. The flows associated with these ducts differ from those in simple annular diffusers both as a consequence of their high-curvature S-shaped geometry and of the presence of wakes created by the upstream turbine. Experimental data and numerical simulations clearly reveal the generation of significant secondary flows as the flow develops through the diffuser in the presence of cross-passage pressure gradients. The further influence of inlet swirl is also demonstrated. Data from experimental measurements with and without an upstream turbine are discussed and computational simulations are shown not only to give a good prediction of the flow development within the diffuser but also to demonstrate the importance of modeling the fully three-dimensional nature of the flow.

Introduction

Interturbine diffusers are increasingly used in the context of gas turbine design to diffuse the flow between the H.P. or I.P. turbine and the L.P. turbine while maintaining surface continuity. Diffusing the flow upstream of the L.P. turbine and increasing the mean passage radius allows higher turbine stage efficiency to be achieved as a consequence of reducing both the flow coefficient and the stage loading coefficient. To avoid unacceptable weight penalties, the diffusion must be achieved in the shortest possible length while preventing boundary layer separation and instability in the rapidly diffusing flow.

Diffuser Flows. Simple diffusers and their associated flows have been well documented (e.g., ESDU, 1976) and the factors influencing their efficiency are predominantly the area ratio of the diffuser and the length of the flow path over which the diffusion occurs. The modification of the local pressure gradients as a result of wall curvature and the consequent influence upon turbulent boundary layer behavior may substantially change the performance of the diffuser, as may turbulence within the wakes from upstream blade rows or other sources. Published data on S-shaped, annular ducts relate mostly to intercompressor passages of reducing radius with local, curvature-induced pressure gradients but little or no overall diffusion. Britchford et al. (1993) showed that the addition of an upstream rotor led to a reduction in the hub boundary layer shape factor in the diffusing zone around the first bend, which they attributed to increased turbulent mixing. Although radial flow migration within the low-energy wakes under the influence of the cross-passage pressure gradient was very weak, the authors concluded that this was responsible for the re-energizing of the hub boundary layer, which consequently reduced its tendency to separate.

Pfeil and Going (1987) observed that the development of the turbulent boundary layers in a straight-cored annular diffuser behind a single compressor stage is greatly influenced by wake propagation. Although their measurements showed a contrast between the essentially two-dimensional boundary layers at midpitch and the strongly three-dimensional nature of the flow in the wake region, the extent of the wake influence remains unknown. A thorough review of the published literature is provided by Dominy and Kirkham (1996).

Only Dominy and Kirkham (1995, 1996), have published comparable data for ducts with both significant diffusion and curvature. Their data confirmed that the flow is strongly influenced by wake propagation and that cross-passage pressure gradients induce radial flows within the wakes, leading to clearly defined secondary flows with their consequent redistribution of loss and significant local yaw and pitch over much of the passage.

Swirling Flows. The local effect of swirl in an annular diffuser is to produce a radial pressure gradient to balance the centrifugal force which increases the static pressure along the casing wall and decreases it at the hub. For a diffusing, swirling flow the pressure coefficient at some axial location x is given by the expression (Lohmann et al., 1979):

$$Cp_x = \left(1 - \frac{\rho_i A_i^2}{\rho_x A_x^2}\right) + \tan^2 \alpha_i \left(1 - \frac{\rho_i r_{i_m}^2}{\rho_x r_{x_m}^2}\right) \qquad (1)$$

The first diffusion term is due to geometric area change and the second results from the conservation of angular momentum in a flow of changing mean radius. If the inlet swirl angle is nonzero, a change of mean radius leads to a static pressure rise even for a constant area duct. The static pressure rise through the diffuser is strongly dependent upon both the inlet swirl angle and the cant angle. Coladipietro et al. (1975) and Kumar and Kumar (1980) both reported that for unstalled, straight-walled annular diffusers the static pressure rise coefficient increased with increasing swirl. Kumar and Kumar (1980) also reported that as the inlet swirl angle was increased, the pressure rise reached a peak and then decayed with further swirl increase. This was attributed to the increased path length, giving rise to increased rotational kinetic energy losses through skin friction. McDonald and Fox (1971) found that the performance of stalled, conical diffusers with an axial inlet flow could be improved by the introduction of swirl, but unlike Kumar and Kumar (1980), he found little benefit from swirl for unstalled flows. Bradshaw (1973) demonstrated that centrifugal and Coriolis body forces alter the turbulent structure of the flow. For swirling flow in an annular passage, the production of turbulent energy is suppressed in the vicinity of the hub wall, where the radial pressure gradient is positive and enhanced near the casing where the gradient relative to the boundary layer is reversed with an implied variation in the rate of growth of the surface boundary layers. The difference in turbulent energy production would suggest that in an annular diffuser inlet swirl would stabilize the casing and destabilize the hub boundary layers.

Contributed by the International Gas Turbine Institute and presented at the 41st International Gas Turbine and Aeroengine Congress and Exhibition, Birmingham, United Kingdom, June 10–13, 1996. Manuscript received at ASME Headquarters February 1996. Paper No. 96-GT-139. Associate Technical Editor: J. N. Shinn.

Table 1 Geometric and operating parameters of the durham S-shaped diffuser rig

Inlet hub diameter	0.286m
inlet casing diameter	0.412m
exit hub diameter	0.551m
exit casing diameter	0.660m
Area Ratio exit / inlet	1.5
Inlet Reynolds Number (based on inlet passage height)	3.9×10^5
Inlet Dynamic Head (nominal)	4.5 kPa
Number of Inlet Swirl Vanes	34
Inlet Free Stream Turbulence	2.5%

This has been confirmed experimentally by Lohmann et al. (1979) who reported premature separation on the hub and Kumar and Kumar (1980) who reported that inlet swirl reduced the likelihood of separation occurring on the casing of stalled diffusers. Hoadley and Hughes (1969) have also shown that separation in a parallel-cored, annular diffuser may be completely suppressed or moved from the normal outer wall location to the inner core depending upon the degree of inlet swirl. For turbines designed to operate with axial exit flow, the evidence suggests that off-design operation with its associated introduction of a small degree of swirl is likely to have a stabilizing effect upon the critical casing flow and is not therefore of major concern during the design process.

In this study the quasi-steady influence of a nonuniform inlet flow arising from wake propagation has been investigated through measurements in the Durham University annular diffuser rig and computations made using the Moore Elliptic Flow Program (MEFP). Inlet swirl angles of 0 and 15 deg were chosen to simulate realistic design and off-design operating conditions, but work is currently in progress to investigate the effect of more extreme degrees of swirl. The additional effects of blade-generated secondary flows and rotation are addressed through measurements made by Rolls-Royce plc in a model turbine test rig.

Experimental Facility

The Durham University Diffuser Rig. The Durham University S-Shaped Duct Facility has been described in detail by Dominy and Kirkham (1995, 1996) and the important geometric and operational parameters are described in Table 1.

The initial duct curvature begins 2.5 inlet passage heights downstream from a row of 34 swirl vanes and the flow is turned radially through a nominal angle of 36 deg. Traversing within the diffuser may be performed at 12 alternative axial positions. Data from four of those traverse planes are presented here and their locations are shown in Fig. 1(*a*). Static pressure tappings are located at each traverse plane on both the hub and the casing and additional tappings are positioned at the points of greatest change of surface pressure gradient. Area traverses were performed using 2-mm-dia, five-hole pressure probes for the bulk of the flow and 0.8-mm-thick, three-hole cobra-type probes close to the walls. The confines of the duct preclude the adoption of probe nulling so a calibration method was adopted allowing flow angles of up to ±40 deg in yaw and pitch to be measured.

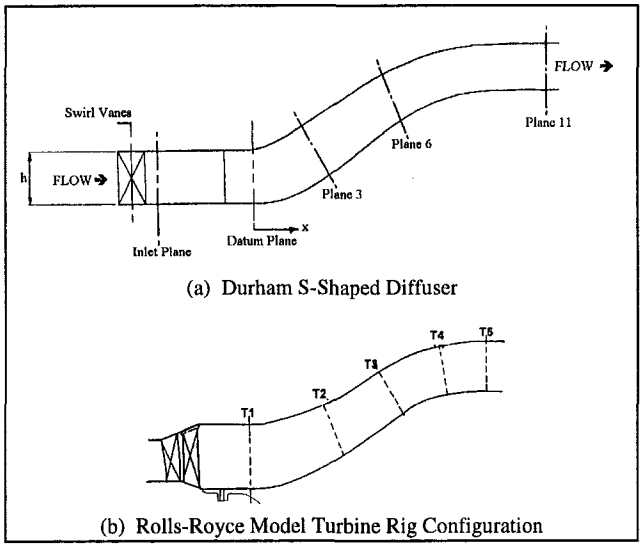

Fig. 1 Traverse plane locations and general geometry of (*a*) the Durham rig and (*b*) the model turbine rig

The probes were calibrated at the operating Reynolds number to minimize potential calibration errors (Dominy and Hodson, 1993) and typical, estimated measurement uncertainties were $0.01q_i$ for stagnation pressure and ±0.8 deg for radial and circumferential flow angle.

The Model Turbine Rig. Measurements in a scaled duct were performed downstream of a single-stage LP turbine in the Rolls-Royce No. 4 Turbine Test Facility (Fig. 4). Measurements were made at a Reynolds number of 3.2×10^5 and at a fixed axial Mach number of 0.23 at the diffuser inlet with a typical, uniform inlet temperature of 370 K. Area traversing was possible at the inlet and exit planes of the diffuser and radial traversing was performed at three intermediate planes. Static pressures were measured along the duct at three alternative circumferential positions to assess circumferential variation. All of the pressure measurements were made using fixed probes and tappings and represent time averages.

CFD

The numerical analysis of the flow was performed using the Moore Elliptic Flow Program, which has been thoroughly described in the published literature (e.g., Moore and Moore, 1985; Moore, 1985). The code solves the Reynolds-averaged Navier–Stokes equations in three dimensions and the elliptic nature of the equations allows reversed flows and hence separations to be indicated. Further details of the application of the code to the particular flows assessed here are provided in the relevant sections of the text.

Results and Discussion

Axial Inlet Flow. Area traverses were performed in the model turbine rig at the inlet and exit planes (planes T1 and

Nomenclature

A = local cross-sectional area
Cp = pressure rise coefficient
L = duct axial length
h = inlet passage height
p = static pressure
P_o = stagnation pressure
q = dynamic head
r = radius
Re = Reynolds number
x = axial distance
α = swirl angle
δ^* = boundary layer displacement thickness
ρ = density

Subscripts

e = exit plane
i = inlet plane
m = mean
n = number of traverse plane
x = local axial position

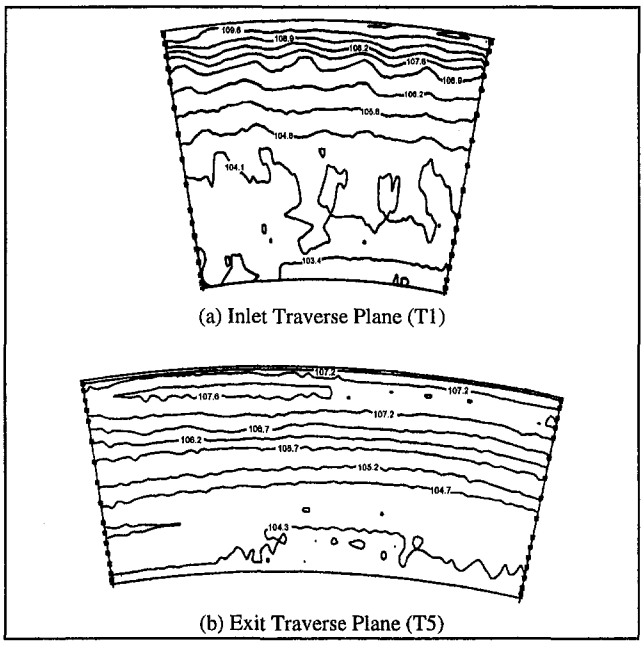

Fig. 2 Turbine rig total pressure contours (kPa) at the inlet and exit planes

T5, Fig. 1(b)) at a Reynolds number of 3.2×10^5 and the corresponding contours of total pressure are shown in Fig. 2. The time-averaged, inlet total pressure traces display reasonable circumferential uniformity although small perturbations are observed. These may be due solely to measurement uncertainty but they may also be associated with asymmetric flow from the upstream NGV's and rotor. No additional data were available to investigate this observation further. The development of the time-averaged hub and casing boundary layers is shown in Fig. 3 together with a numerical calculation based upon a circumferentially uniform inlet flow, which was matched to the measured data. The calculations were performed using 76 axial planes and 41 radial planes using both the Baldwin–Lomax model (presented here) and an alternative one-equation model. In this

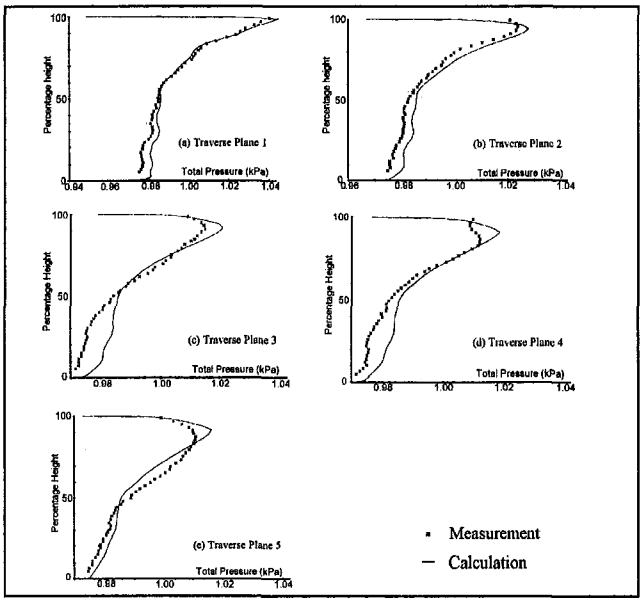

Fig. 3 Total pressure profile development through the turbine rig with an upstream stage

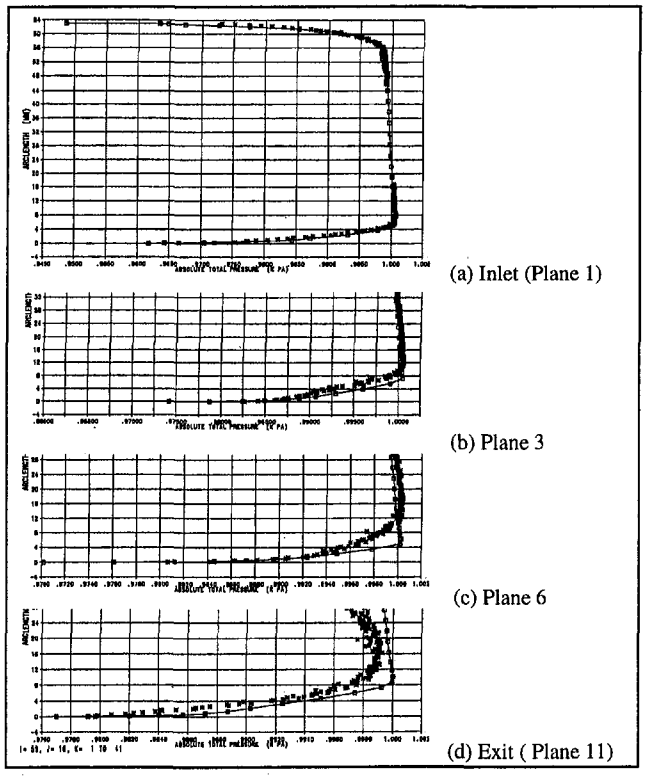

Fig. 4 Durham rig (no swirl vanes): total pressure [measurement; –□– prediction]**

diffuser the boundary layers are always fully turbulent and no differences were apparent between calculations using the two turbulence models.

At the exit traverse plane the simulation displays a good likeness to the measured data but the development of the flow upstream from the exit shows errors particularly near the hub where the calculation overpredicts the total pressure. With the same computational grid and turbulence model, predictions of the near-hub flow in the Durham rig more closely match the experimental data (Fig. 4) suggesting underlying differences in the flows through the two rigs. The Durham rig provides a much simplified inlet flow (Fig. 4(a)), which helps to clarify the development of the flow through the diffuser.

The slight total pressure gradient that is observed is due to a small velocity gradient at the plane of the inlet turbulence grid and the increasing scatter in the data through the duct arises from slight unsteadiness created in the inlet contraction which is exaggerated in the diffusing flow.

In the turbine rig the inlet flow angle is nominally zero, but it may be seen from Fig. 5 that locally the swirl may deviate from the mean by almost 20 deg. However, there are more

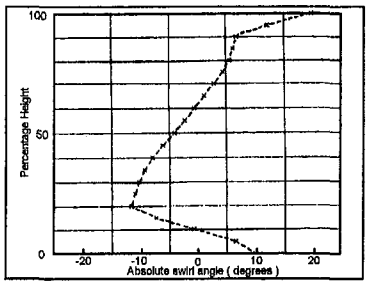

Fig. 5 Turbine rig: radial variation of circumferentially averaged swirl angle (measurement)

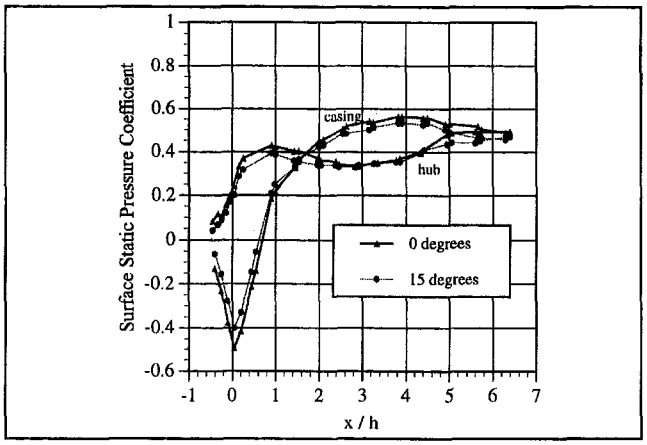

Fig. 6 Axial surface static pressure distribution with and without swirl (measurement, Durham rig)

fundamental differences in the inlet flows of the two rigs. These relate to the flows generated by and through the upstream stage, i.e., the effects of blade wakes from the stator and rotor, secondary flow vortices and periodic, rotating wake–wall interactions. Predictions of the rotor wake influence upon the flow through the turbine test rig suggest that for this application, the wake pressure and velocity deficit have largely dissipated by the plane of entry of the diffusing duct but there are no equivalent unsteady measurements for validation. To allow the first step in a parametric study of these flows, the Durham rig has been tested with representative wakes passing along the duct. The wakes were generated by a fixed row of guide vanes situated 0.85 passage heights upstream of the geometric entry to the diffuser. The term geometric entry is used to emphasize that the presence of the diffuser has an influence upon the local static pressure profile that extends upstream from this point. The development of the inlet flow in the absence of inlet swirl and the development of that flow through the duct has been fully described by Dominy and Kirkham (1994) and is briefly summarized below.

The pressure distribution though the duct (Fig. 6) clearly demonstrates zones of strong diffusion and cross-passage pressure gradients and the most rapid diffusion occurs where the influences of the wall curvature and the rapidly increasing duct area are additive. Dominy and Kirkham (1996) have shown that in the absence of wake propagation, this pressure distribution provides a severe but well-behaved test case in which the boundary layers remain attached at the design flow condition.

The inlet wake structure shows only very minor interaction between the wake and the wall boundary layers (Fig. 7). As the flow passes around the first bend the pressure gradient between the hub and the casing leads to a radially outward flow component within the low-energy wake. By traverse plane 3

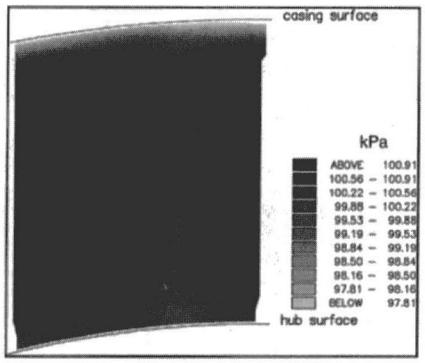

Fig. 8 Measured total pressure contours (plane 3, $x/h = 1.17$, zero swirl)

(nominal $x/h = 1.169$) the cross-passage driving pressure gradient has fallen from a peak of almost 65 percent of the inlet dynamic head to about 20 percent. Total pressure contours (Fig. 8) show a slight broadening and weakening of the wake relative to the inlet flow and also a thickening of the casing boundary layer. By plane 6 (nominal $x/h = 2.62$) the strong adverse pressure gradient on the casing downstream from the first curvature has resulted in further boundary layer growth, which is exaggerated by the radially outward flow of low energy fluid that has occurred within the wakes (Fig. 9).

As the flow is turned back toward the axial direction, the sign of the radial pressure gradient reverses, reaching a peak cross-passage pressure difference corresponding to 20 percent of the inlet dynamic head. Plane 11 ($x/h = 5.57$) lies in the parallel section of the duct downstream from the second bend where the cross-passage pressure difference has decayed almost to zero. The cumulative influence of the zone of reversed pressure gradient does not significantly influence the three-dimensional character of the flow that has developed (Fig. 10(a)) and the remaining wake is very weak. Vortices are observed either side of the wake at both the hub and the casing (Fig. 10(b)) but the casing vortices are both larger and stronger. One influence of the secondary vortices is to accumulate loss close to the wall but away from the wake axis. The asymmetry of the flow suggests that there must have been some inlet asymmetry or swirl, which has been exaggerated as the diffusing flow developed. Despite the growth of the wake-induced secondary flows, their influence upon the overall performance of the diffuser is remarkably slight in terms of both pressure recovery and loss generation with the changes lying close to the limits of experimental accuracy. No change in the surface static pressure distribution is observed relative to the wake-free case, which implies that the three-dimensional flows result primarily in a redistribution of the inlet loss and not a creation of additional loss. In view of these wake-induced secondary flows, it is not surprising to find that CFD analysis of the flow in the turbine rig based upon a circumferentially averaged inlet flow results

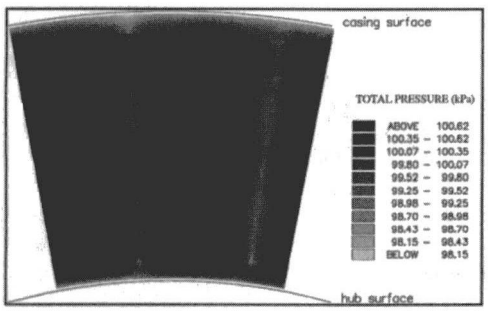

Fig. 7 Measured inlet total pressure contours (Durham rig, inlet guide vanes fitted, zero swirl)

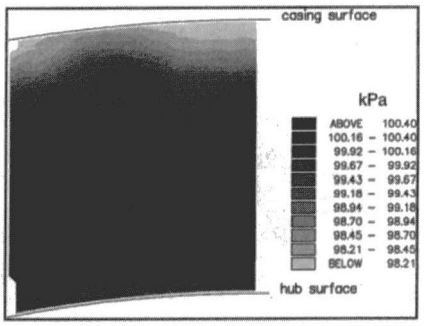

Fig. 9 Measured total pressure contours (plane 6, $x/h = 2.62$, zero swirl)

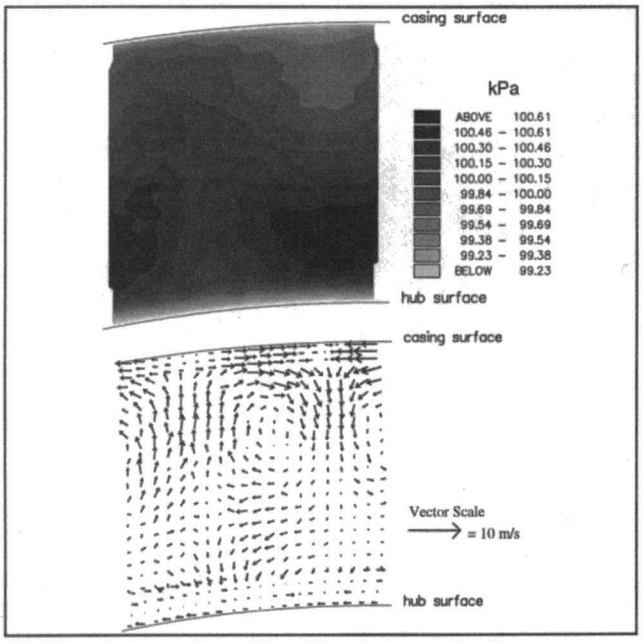

Fig. 10 Total pressure contours and secondary velocity vectors (measurement plane 11, x/h = 5.57, zero swirl)

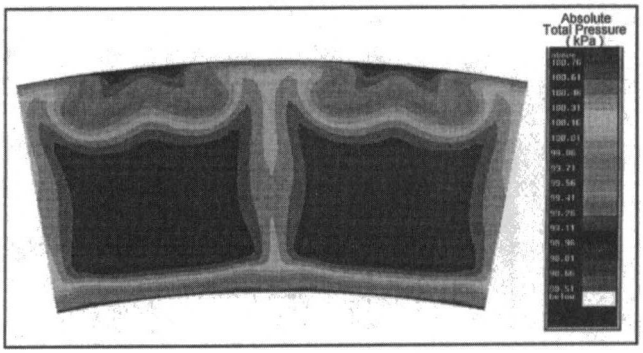

Fig. 12 Predicted exit total pressure contours (plane 11, swirl vanes set for zero swirl)

in a maldistribution of the pressures and losses. The diffuser flow within the Durham rig has therefore been analyzed to investigate the simulation of the wake-induced flows arising from the fixed inlet guide vanes. The computational mesh comprised 76 axial grid points and 41 radial points (matching the two-dimensional calculations) and 31 circumferential grid points over one guide vane pitch. The inlet flow conditions were matched exactly to the measured data. Figure 11 shows the development of the total pressure profile at different circumferential locations at each of the four sample traverse planes and the circumferential nonuniformity of the flow is clearly evident. The predictions are compared with the radial profiles measured midway between the inlet guide vanes wake axes and here the measured data indicate a more mixed-out flow than the prediction. However, it has been discovered that the plane where the inlet traverse was measured was farther upstream of the calculation grid inlet than was believed at the time of the calculations so some additional mixing will be evident in the measured data. Comparing the measured exit flow (Fig. 10) with the MEFP prediction (Fig. 12), similar trends are observed. The prediction shows stronger secondary flow vortices and less inward migration of the casing boundary layer, indicating less mixing. This will be influenced by the mismatched inlet lengths described above but may also be a function of the chosen turbulence model. The latter influence requires further investigation.

15 deg Inlet Swirl. Predictions of the flow development through the duct with inlet swirl show similar trends when compared to experimental data. Figure 13 demonstrates the loss generation and redistribution as the flow progresses through the diffuser. With the introduction of inlet swirl, the wake breadth increases due to stalling of the guide vanes and a relative thinning of the wake near the walls is observed arising from secondary flow creation at the vane tips. The untwisted inlet guide vanes generate an almost uniform inlet yaw angle across the passage in the bulk flow but the wake axes are no longer truly radial.

A full discussion of the inlet flow and its development is provided by Dominy and Kirkham (1995), but the important observations are summarized here. On turning through the initial, radially outward bend the skew of the wakes is exaggerated and by plane 3 (x/h = 1.17) the wakes remain clearly defined but strongly skewed, as shown by both the numerical prediction and by measured total pressure data (Fig. 14). By plane 6 (x/h = 2.62) the radial pressure gradient has reversed but remains relatively week. Here the wakes are observed to have skewed further and the high-loss fluid that is associated with those wakes has almost entirely accumulated at the casing. The vortical motion that continued to drive the flow against the cross passage pressure gradient in the axial case (Dominy and Kirkham, 1996) is much reduced in the absence of any significant

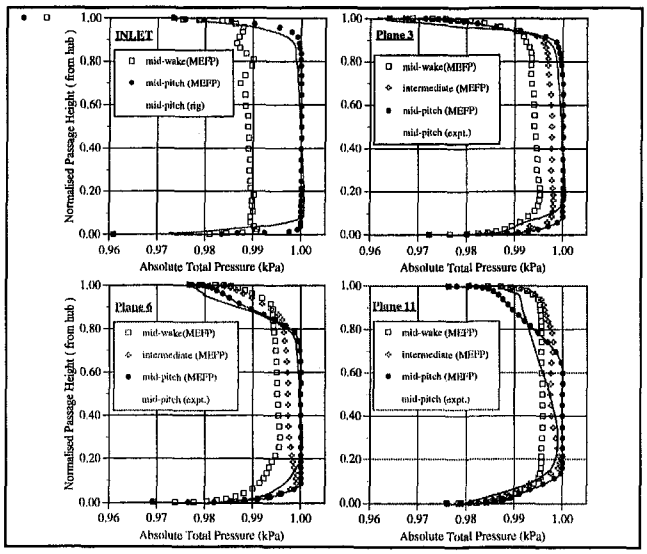

Fig. 11 Predicted radial distribution of total pressure at different circumferential positions with measured, midpitch data

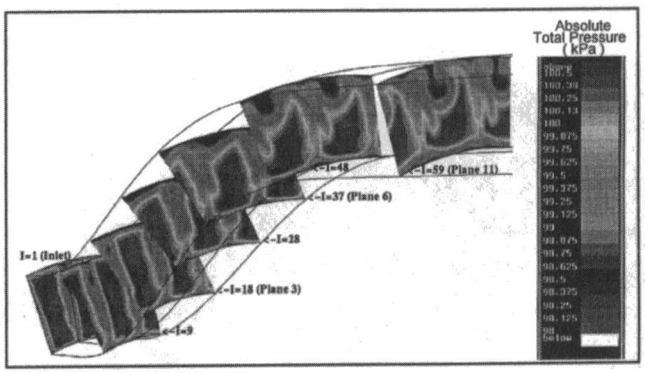

Fig. 13 Predicted development of the total pressure distribution through the diffuser (15 deg inlet swirl)

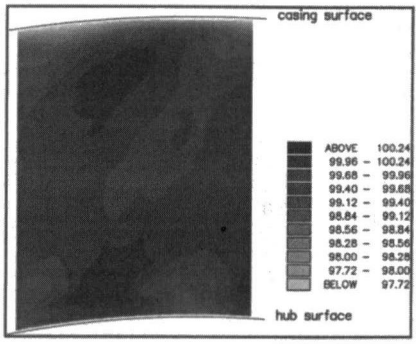

Fig. 14 Measured total pressure contours (traverse plane 3, $x/h = 1.17$, 15 deg swirl)

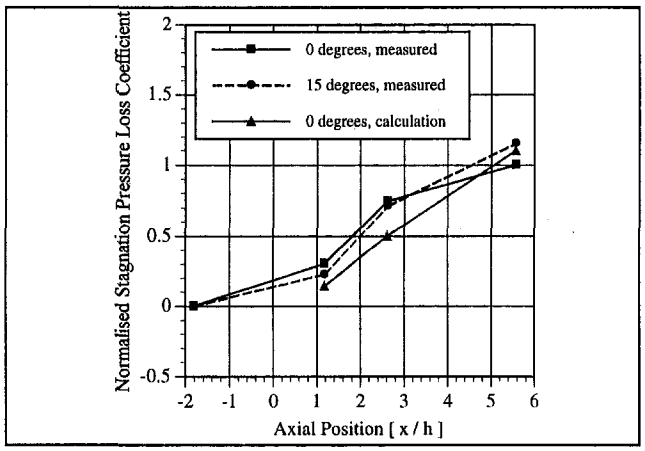

Fig. 16 Loss development with and without swirl

radial flow component in the wake. As a consequence the form of the casing "boundary layer" is as much due to the merging of the natural boundary layer and the wake as to the classical growth of the wall boundary layer.

Figure 15 shows a pronounced vortex associated with the loss core at plane 11, but its character differs significantly from the zero swirl case where the velocity vectors provide clear evidence of four vortices with a stronger, counterrotating pair lying symmetrically either side of the wake near the casing and a much weaker pair in the hub side of the passage. In the swirling flow, the skew of the wakes and the relative circumferential shift of the casing vortex pair relative to the hub pair appears to result in the merging of the hub and casing vortices of the same sign albeit with the casing side vortex clearly the dominant partner.

Despite the observed differences in the detail of the flow structures within the duct under the influence of swirl, their influences upon the overall performance of the diffuser are surprisingly small with little difference observed in the exit static pressures (Fig. 6). As a result of the effective reduction of wall curvature that is experienced by the swirling flow, the magnitude of the static pressure coefficient at the point of maximum velocity is reduced by 20 percent and a similar reduction is observed in the hub diffusion around the first bend. The loss generation through the duct also remains little changed by the presence of swirl. Figure 16 shows the normalized increase of stagnation pressure loss through the duct for both the zero swirl and 15 deg swirl cases. Each data point shows the loss generated within the duct (downstream from the inlet traverse plane) based on inlet dynamic head normalized against the mixed out exit loss value for the zero swirl case, i.e.,

$$\text{normalized loss} = \left[\frac{P_{0,x} - P_{0,i}}{(P_0 - p)_i}\right] \div \left[\frac{P_{0,e} - P_{0,i}}{(P_0 - p)_i}\right]_{\text{zero swirl}} \quad (2)$$

The loss grows most rapidly between the bends and the overall loss increases with swirl as a consequence of the increased path length. The measured distribution of the loss indicates that the initial loss is reduced with swirl, which is probably a consequence of the initial radial pressure gradient being more favorable and thus mixing is reduced. Up to the second bend and beyond, the pressure gradients increase with swirl, promoting more mixing and hence loss. The overall predicted loss compares well with the measured loss, although ahead of the second bend the measured loss is higher than that predicted. This may be due to the discrepancies between the calculation and measurement at the inlet plane and also to the accuracy of the turbulence model. Overall MEFP gives a good prediction of the duct flow with wakes. The effect of the shorter calculation inlet length is probably only secondary, since it will be the diffusion and curvature in the duct that will have the greatest effect upon the loss generation.

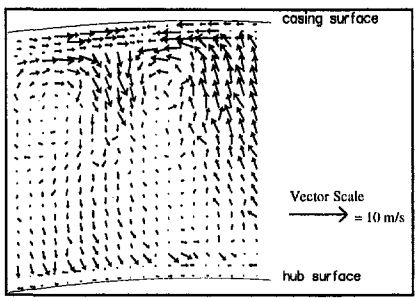

Fig. 15 Measured secondary velocity vectors (traverse plane 11, $x/h = 5.57$, 15 deg swirl)

Conclusions

The influence of wakes and swirl upon the flow through a diffusing, S-shaped duct is shown to have a significant effect upon the detailed structure of the flow. Secondary flows resulting from the influence of cross-passage pressure gradients upon the low-energy wake and boundary layer flows are clearly evident with their associated redistribution of loss and local variations in yaw and pitch. Swirl is shown to influence the character of the flow particularly through the skewing of the wakes as they pass through the diffuser. This is observed to change the distribution of loss within the duct, although the evidence suggests that this is mostly a redistribution of the loss generated near the wall and of the loss already present in the inlet flow. Computational simulations generally give a good prediction of the flow development within the diffuser and of the loss generation when the truly three-dimensional nature of the flow is represented. Calculations based upon a circumferentially averaged inlet flow show clear limitations.

Acknowledgments

The work described was supported by the Defence Research Agency and Rolls-Royce plc. The assistance of their representatives and their permission to publish the work described in this paper is gratefully acknowledged.

References

Bradshaw, P., 1973, "Effects of Streamline Curvature on Turbulent Flow," AGARD AG-169.

Britchford, K. M., Manners, A. P., McGuirk, J. J., and Stevens, S. J., 1993, "Measurement and Prediction of Flow in Annular S-Shaped Ducts," *Proc. 2nd International Symposium on Engineering Turbulence Modelling and Measurements*, Florence, Italy, pp. 785–794.

Coladipietro, R., Schneider, J. H., and Sridhar, K., 1975, "Effects of Inlet Flow Conditions on the Performance of Equiangular Diffusers," *Trans. CSME,* Vol. 3, No. 2, pp. 75–82.

Dominy, R. G., and Hodson, H. P., 1993, "An Investigation of Factors Influencing the Calibration of Five-Hole Probes for Three-Dimensional Flow Measurements," ASME JOURNAL OF TURBOMACHINERY, Vol. 115, pp. 513–519.

Dominy, R. G., and Kirkham, D. A., 1995, "The Influence of Swirl on the Performance of Inter-Turbine Diffusers," VDI Berichte No. 1186.

Dominy, R. G., and Kirkham, D. A., 1996, "The Influence of Blade Wakes on the Performance of Inter-Turbine Diffuser," ASME JOURNAL OF TURBOMACHINERY, Vol. 118, pp. 347–392.

ESDU, 1976 (amended 1990), "Introduction to Design and Performance Data for Diffusers," Engineering Science Data Unit data item 66027, ISBN 0 85679 164 4.

Hoadley, D., and Hughes, D. W., 1969, "Swirling Flow in an Annular Diffuser," Report CUED/A-Turbo/TR5, Department of Energy, University of Cambridge, United Kingdom.

Kumar, D. S., and Kumar, K. L., 1980, "Effect of Swirl on Pressure Recovery in Annular Diffusers," *Journal of Mechanical Engineering Science,* Vol. 22, No. 6, pp. 305–313.

Lohmann, R. P., Markowski, S. J., and Brookman, E. T., 1979, "Swirling Flow Through Annular Diffusers With Conical Walls," ASME *Journal of Fluids Engineering,* Vol. 101, No. 2, pp. 224–229.

McDonald, A. T., and Fox, R. W., 1971, "Effects of Swirling Flows on Pressure Recovery in Conical Diffusers," *AIAA Journal,* Vol. 9, No. 10, pp. 2014–2018.

Moore, J. G., 1985, "An Elliptic Calculation Procedure for Three-Dimensional Viscous Flow," AGARD-LS-140 4.1–4.16.

Moore, J., and Moore, J. G., 1985, "Performance Evaluation of Linear Turbine Cascades Using Three-Dimensional Viscous Flow Calculations," ASME *Journal of Engineering for Gas Turbines and Power,* Vol. 107, No. 4, pp. 969–975.

Pfeil, H., and Going, M., 1987, "Measurements of the Turbulent Boundary Layer in the Diffuser Behind an Axial Compressor," ASME JOURNAL OF TURBOMACHINERY, Vol. 109, pp. 405–412.